Algorithms for fitting cylindrical objects to sparse range point clouds for rapid workspace modeling

Soon-Wook Kwon
GRA/Field Systems and Construction Automation Lab., The University of Texas at Austin, Austin, TX 78712-0276 USA (e-mail: swkwon@mail.utexas.edu)
Katharine A. Liapi
Assistant Professor, The University of Texas at Austin, Austin, TX 78712-0276 USA (e-mail: kliap@mail.utexas.edu)
Carl T. Haas
Professor, The University of Texas at Austin, Austin, TX 78712-0276 USA (e-mail: haas@mail.utexas.edu)
Frederic Bosche
GRA/Field Systems and Construction Automation Lab., The University of Texas at Austin, Austin, TX 78712-0276 USA (e-mail: bosche.frederic@mail.utexas.edu)

ABSTRACT: Current methods for construction site modeling employ large, expensive laser range scanners that produce dense range point clouds of a scene from different perspectives. While useful for many purposes, this approach is not feasible for real-time applications, which would enable automated obstacle avoidance and semi-automated equipment control, and could improve both safety and productivity significantly. This paper presents human-assisted rapid environmental modeling algorithms for construction, and focuses on cylindrical object fitting algorithms. The presented algorithms address construction site material of cylindrical shape. Experiments were conducted to determine: (1) the effect of the ratio of length to diameter of the cylinder to the accuracy of the results, (2) the effect of the angle of view to the accuracy of the results, (3) the minimum number of scanned points required to give adequate modeling accuracy for cylinders of various length to diameter ratios. The results indicate that the proposed algorithms can model geometric primitives used in a construction site rapidly and with sufficient accuracy for automated obstacle avoidance and equipment control functions.

KEYWORDS: CONSTRUCTION AUTOMATION; LASER RANGE FINDER; OBJECT FITTING; OBJECT MATCHING; WORKSPACE MODELING

1. INTRODUCTION

Considerable effort has been devoted to the development of methods of extracting geometrical information from a scene, which is still a major concern for both computer vision and robot vision (Lebegue 1993, Tsukiyama 1996). Determining the dimensions, distance and orientations of planar and curved object surfaces such as wall, doors, pipes and other man-made objects is still a key issue and therefore modeling of the geometric features of a workspace typically demands a large amount of computation due to very large data sets (Tsukiyama 1996). A new method to extract geometric information from a scene by taking advantage of human cognitive skills is under development at the University of Texas at Austin (Cho et al 2002, Kwon et al 2002). A significant advantage of this approach is the ability to extract models of real world objects in a construction workspace from only a limited number of scanned points (less than 50 pts. per object),which are termed sparse point clouds here.

Current methods for construction site modeling employ large, expensive laser range scanners that produce dense range point clouds of a scene from different perspectives. While useful for many purposes, this approach is not feasible for real-time applications, which would enable automated obstacle avoidance and semi-automated equipment control, and could improve both safety and productivity significantly (McLaughlin 2002). The dynamic nature of the construction environment requires that a real-time local area modeling system be capable of handling a rapidly changing and uncertain work environment. However, in practice, simple, and reasonably accurate geometric primitives can give a sufficient feedback to an operator, who is controlling an equipment to place objects in an unstructured construction site. For real-time obstacle avoidance, such volumes also facilitate computational tractability.

With regard to the geometric objects most frequently encountered in a workspace, it appears

that a few types of primitives can be used to model a wide range of construction scenes. These are planar objects, cuboids, and cylindrical objects. Particularly, cylindrical objects can be used in plant construction to fit and match chemical pipes, ventilation pipes, and plumbing pipes. This paper presents algorithms that accurately fit and match objects of cylindrical shape, with regard to location and orientation, to sparse point clouds. Experiments were conducted to determine modeling accuracy of the algorithm at the Field Systems and Automation Laboratory of The University of Texas at Austin.

2. THE FITTING METHOD FOR CYLINDRICAL OBJECTS

A single-axis laser range finder, a pan/tilt unit (PTU), and a personal computer were used for the experimental set up. The single-axis laser range finder (DistoMemo) that is mounted on the PTU is designed not only for hand-held operation, but also for computer use through an interface. The measurements can be remotely taken and transferred directly into the computer.

Recent research results indicate that graphical workspace modeling can improve construction equipment control and operations. Equipment operators can use graphical workspace models as an interactive visual feedback tool while controlling equipment (Kim and Haas 2000). For the rapid modeling of construction site objects from sparse point clouds three basic algorithms have been developed that address construction site objects. These are: (1) cuboid fitting algorithm, (2) cylinder fitting algorithm, (3) sphere algorithm, and (4) planar algorithm. This paper focuses on the cylinder fitting algorithm.

Algorithm development and revisions were based on lab experiments. By using these algorithms we achieve: (1) accurate and reliable methods to save computational cost and time, (2) improved fitting algorithms to attain real-time execution, and (3) increased modeling accuracy with operator's assistance. Figure 1 shows the entire fitting process.

2.1 Solid cylinder fitting algorithm

Four parameters are necessary to define a bounded cylinder: *a* scalar radius *r*; an axis vector, *a*; a center point to place the axis vector, *c* = (*Xc, Yc, Zc*); and a length of cylinder that defines the boundary of the cylinder. This algorithm uses the nearest neighbor algorithm to define the normal vector. Four scanned points are used to compute the planar surface of the cylinder. By projecting the points on the curved surface onto the computed planar surface, parameters *r* and *c* can be estimated. The radius of the circle is defined as the distance from the center of the circle to any point on the optimized curve. A primary estimation of the radius, ř, is found by $\check{r} = mean\ (|\hat{c} - k'|)$ (k' = {the projected points on the optimized curve of planar surface}). Consequently the final values of *a, c, r* are found by the least squares method using data *d*.

2.2 Hollow cylinder fitting algorithm

In the hollow cylinder fitting algorithm, Principal Components Analysis (PCA) was used to determine the primary axis of cylinder. Excluding the steps for computing the primary axis, the other steps of the algorithm follow the same sequence as the solid cylinder algorithm.

PCA is a distribution-based ordination method in which the distance between sites in an ordination diagram is correlated with multi dimensional distribution (Duda et al, 2001). PCA assumes that all vectors in a set of n dimensional samples $a_1 \ldots a_n$ can be explained by a single vector a_0. The vector a_0 is derived using the least squares method, in which the sum of the squared distances between a_0 and the various a_k are minimized. We define the square-error criterion function $F_0(a_0)$ by

$$F_0(a_0) = \sum_{b=1}^{n} \left\| a_0 - a_k \right\|^2 \tag{1}$$

$$p = \frac{1}{n} \sum_{b=1}^{n} a_b \tag{2}$$

$$F_0 = \sum_{b=1}^{n} \left\| (a_0 - p) - (a_b - p) \right\|^2 \tag{3}$$

Projecting the sample data onto a line through the sample mean, one-dimensional representation can be computed. If we let *e* be *a* unit vector of the line direction, the line equation is

$$a = p + de \tag{4}$$

Scalar *d* is the distance between the sample data and the sample mean *p*. We can find the coefficients d_k by minimizing the squared criterion function.

$$F_0(d_1, \ldots, d_n, e) = \sum_{b=1}^{n} \left\| (p + d_b e) - a_k \right\|^2 \tag{5}$$

$$d_b = e^t (a_b - p) \tag{6}$$

The best direction e of the line can be found by solving scatter matrix *U*, which is defined by

$$U = \sum_{b=1}^{n} (a_b - p)(a_b - p)^t \tag{7}$$

$$F_1(e) = -e^t U e + \sum_{b=1}^{n} \|a_b - p\|^2 \tag{8}$$

LaGrange multipliers can be used to maximize the *etUe*, which is subject to the constraint ||*e*||=1. Let φ be an undetermined multiplier. We can do the differentiation of

$$v = e^t U e - \phi(e^t e - 1) \tag{9}$$

with regard to *e* getting

$$\frac{\partial u}{\partial e} = 2Ue - 2\phi e \tag{10}$$

By setting the gradient vector equal to zero, we see that *e* should be an eigenvector of the scatter matrix. The eigenvector will be the primary axis of the cylinder that can be obtained by reducing the dimensionality of the feature space and by restricting attention to the directions along the scatter of the cloud (Vemuri et al.1986, Vemuri and Aggarwal 1987, Schweikert 1966). It will be the primary axis of the cylinder.

$$Ue = \phi e \tag{11}$$

After finding the primary axis of a cylinder, the estimated planar surfaces can be generated on the top and bottom of a hollow cylinder. By projecting the points of the curved surface onto the planar surfaces, the radius and center point of the hollow cylinder can be estimated. The radius of the circle is found using the same method used in the solid cylinder algorithm. Consequently the final values of the radius, length, center point, and primary axis are found by this fitting algorithm using scanned data. Figure 2 shows the scanned points and the computed primary axis of the cylinder. Figure 3 illustrates scanned points and projected points onto planar surface of the cylinder. Figure 4 shows the points projected from the curved surface onto the planar surface of the cylinder. Figure 5 shows modeled cylinders computed by the scanned points from actual objects.

3. EXPERIMENTAL RESULTS

Experiments were conducted to determine: (1) the effect of the ratio of radius to length (L/D) of the cylinder to the accuracy of the results, (2) the effect of the angle of view to the accuracy of the results, (3) the minimum number of scanned points required to give adequate modeling accuracy for cylinders of various length to diameter ratios.

Experiments were performed for cylinders with 3-inch through 5-inch radii. For each size of cylinder, several measurements have been conducted. Specifically, measurements based on 10, 20, 30 and 40 scanned points, were conducted for each tested cylindrical object. To increase the accuracy of the experiments, each test has been repeated 30 times. Thus, 120 tests per factor were conducted for the evaluation of the performance of the algorithm in respect to each one of factors (radius, length, and axis). The following results were obtained (Table 1, Figures 6 and 7):

- The relationship between radius and length of the visible section of a cylinder affects the accuracy of the cylinder fitting algorithm
- The most accurate results in radius, length, and axis were obtained for a 90 degree angle of view.

Results of tests using fixed radius (3 to 5-inch), various lengths (range from 10 to 25–inch), and various angles (30, 60, 90 degrees) show that:

- Ten scanned data points give adequately accurate estimates of radius, length, and axis for all tested cylinders.
- Minimal improvement in accuracy is achieved by scanning more than 10 points.

With respect to the accuracy of the estimates of length, both the number of data points and the way scanned data points are distributed on the surface of the cylindrical object play a significant role. In other words, it is of prime importance to select well distributed points on the visible surface of cylinder. Restriction of points only on a small area of the cylinder's surface results in lower correlations and poorer parameter estimates. In addition, the distance from the object to the laser scanner affects modeling accuracy, precision error, and accuracy error.

4. CONCLUSION

The proposed algorithms for fitting cylindrical objects are computationally efficient and suitable for use in equipment control and obstacle avoidance for safety applications. They are also acceptable for generating construction as-builts, however for long pipe sections they would have to be corrected with pipe end points. These algorithms should be broadly applicable.

5. ACKNOWLEDGEMENTS

This paper is based on the research funded by the National Science Foundation (Grant#: CMS-0000137) and the National Institute Standard and Technology (Project NBR: NA1341-02-W-0742). The authors gratefully acknowledge their financial support and encouragement throughout this study. The authors also appreciate the assistance from Sang-Wook Han, J.K. Aggarwal, and Mohan Sridharan.

6. REFERENCES

McLaughlin, J., "Rapid Human-assisted Creation of Bounding Models for Obstacle Avoidance in Construction" Master's thesis, Department of Mechanical Engineering, University of Texas at Austin, Austin, Texas, 2002

Kim, Y., and Haas, C., "A Model for Automation of Infrastructure Maintenance Using Representational Forms," J.of Automation in Construction, Elsevier, pp.57-68, October 2000.

Lebegue, X., Aggarwal, J. K., "Extraction and interpretation of semantically significant line segments for a mobile robot," Proceedings of Robotics and Automation, pp 1778 -1785, May 1992.

Tsukiyama, T., "Understanding man-made environments using nonstructured lighting-3D world modeling for indoor mobile robots," Intelligent Robots and Systems, IROS '97, Proceedings of the 1997 IEEE/RSJ International Conference, Volume: 3, pp 1250 -12577, September 1997.

Cho, Y., Haas, C. T., Liapi, K., and Sreenivasan, S. V., "A Framework for Rapid Local Area Modeling for Construction Automation." Journal of Automation in Construction, 11(6), pp. 629-641, 2002.

Kwon, S., "Human-assisted Object Fitting to Sparse Cloud Points for Rapid Workspace Modeling in Construction Automation", Proceedings of the 19th International Symposium on Automation and Robotics in Construction (ISARC), pp 357-362, September 2002

Duda, R., Hart, P., Stork, D., "Pattern Classification," Wiley-Interscience, 2nd edition, October 2000.

Vermuri, B.C, Aggarwal, J. K., "Representaion and Recognition of Objects from Dense Range Maps," IEEE Trans. on Circuits and Systems, Vol. CAS-34, No. 11, November 1987.

Vermuri, B.C., Mitiche, A., and Aggarwal, J. K., "Curvature-based Representation of Objects from Range Data," Image and Vision Computing, Vol. 4, no. 2, pp. 107-114, 1986

Schweikert, D. G., "An Interpolation Curve Using Spline under Tension," Journal. of Math. Phys., Vol 45, pp312-317, 1966

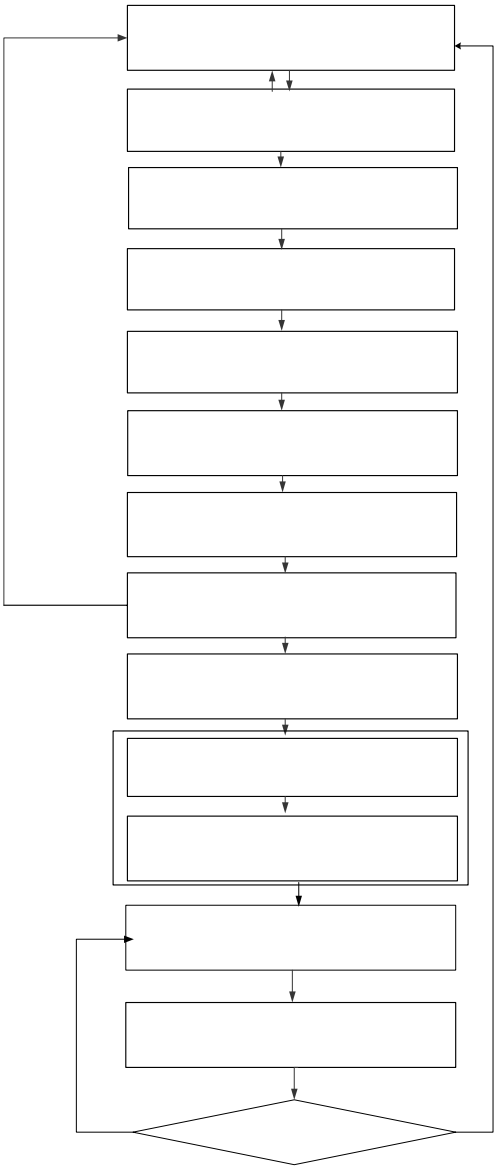

Figure 1 .Object Fitting Method

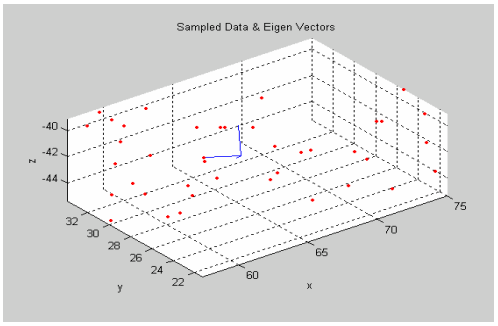

Figure 2. Scanned Points Computed Primary Axis

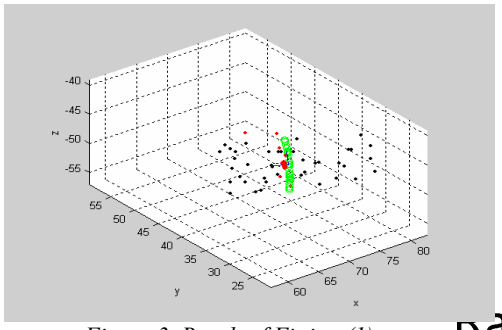

Figure 3. Result of Fitting (1)

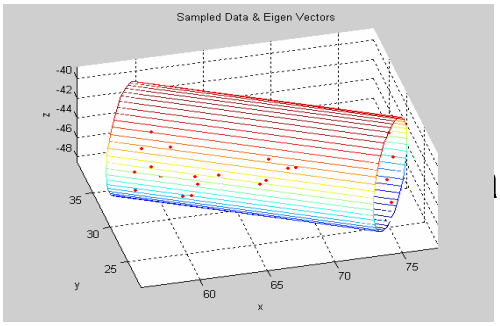

Figure 4. Result of Fitting (2)

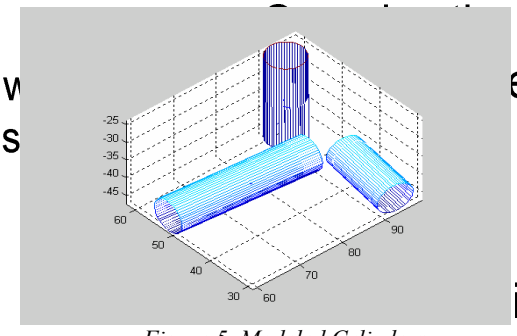

Figure 5. Modeled Cylinders

Scannin

Signal

Range data

nge data

points by

est neigh

ing surfac

Fitting th

Loop until w

modeling is

Table 1. Summary of Experimental Results of Analysis

	10 pts.			20 pts			30 pts			40 pts		
	Percentage of Error (%)			Percentage of Error (%)			Percentage of Error (%)			Percentage of Error (%)		
	Radius	Length	Devi. of Axis	Radius	Length	Devi. of Axis	Radius	Length	Devi. of Axis	Radius	Length	Devi. of Axis
L/D ≈ 1.0	11.50	11.00	14.19	14.50	14.40	15.68	15.50	12.20	20.89	21.50	16.80	24.43
L/D ≈ 1.5	4.75	8.67	2.66	3.75	5.33	2.58	3.50	5.13	2.51	3.50	4.87	2.41
L/D ≈ 2.0	4.50	5.35	2.58	4.00	5.30	2.54	3.50	4.40	2.52	3.50	3.85	2.52
L/D ≈ 2.5	3.00	2.88	1.94	3.00	2.84	1.80	2.75	2.84	1.78	2.00	2.24	1.49

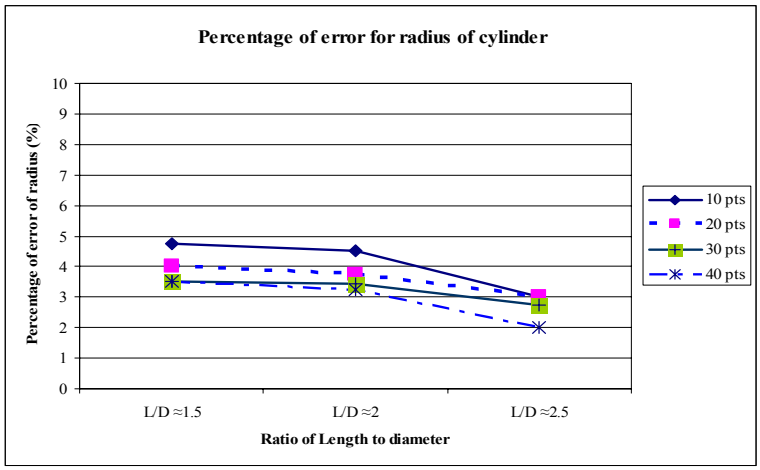

Figure 6. Percentage of Error for Radius of Cylinder

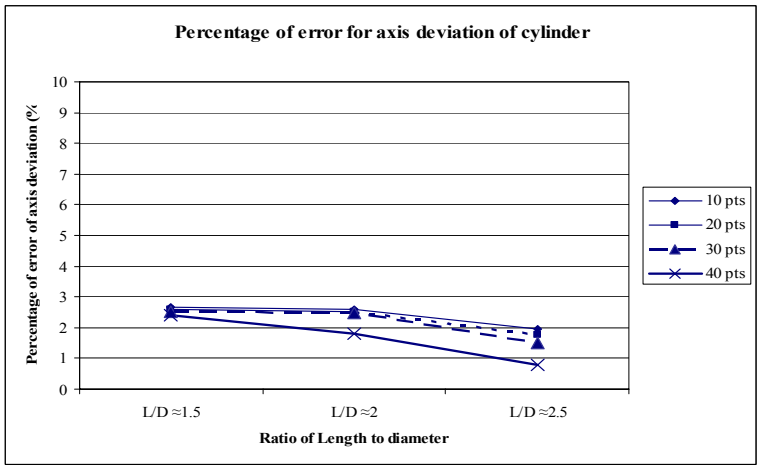

Figure 7. Percentage of Error for Axis Deviation of Cylinder